

Experimental evidence of charge-exchange recombination of highly ionized iron and titanium in Princeton large torus

S. Suckewer, E. Hinnov, M. Bitter, R. Hulse, and D. Post

Princeton Plasma Physics Laboratory, Princeton University, Princeton, New Jersey 08544

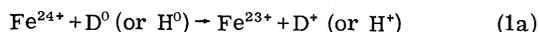
(Received 11 February 1980)

The observed behavior of the emissivities of boronlike Fe XXII, lithiumlike Fe XXIV and Ti XX, and the heliumlike Fe XXV ions in the Princeton large torus tokamak during high-power neutral (H^0 or D^0) beam heating is described. A substantial lowering of the dominant ionization state in the center of the discharge, while the electron temperature is rising, is attributed primarily to increased recombination rate of the ions through charge exchange with neutral hydrogen. This interpretation is supported by the different space and time behavior of the lithiumlike and boronlike ions of comparable ionization potentials, and by comparisons of neutral beam heating of the plasma with ion cyclotron resonance heating, which does not appreciably change the neutral hydrogen concentration. The observations are compared with approximate zero-dimensional model calculations, using experimental plasma conditions and estimated charge-exchange rates.

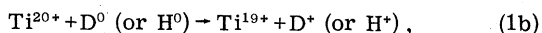
I. INTRODUCTION

During high-power neutral beam injection experiments^{1,2} in the Princeton large torus (PLT), it was observed that the intensity of the resonance lines of the lithiumlike Fe XXIV, and to a somewhat lesser extent the berylliumlike Fe XXIII ions increased by a large amount—considerably more than the general iron concentration increase deduced from the behavior of lower ionization states. The large intensities during the beam injection allowed high-resolution Doppler temperature measurements with these lines,^{1,2} as well as unambiguous identifications and precise wavelength measurements of the corresponding titanium, chromium, and nickel ions,³ which show qualitatively the same behavior.

In three- or four-beam experiments in PLT (Fig. 1) about 2 MW of 40-keV H^0 or D^0 atoms are injected for 0.1 s into a target plasma, with initial central electron temperature about 2 keV and density about $2-3 \times 10^{13} \text{ cm}^{-3}$. As a result the near-central toroidally averaged neutral hydrogen density increases to $\geq 10^8 \text{ cm}^{-3}$, while the plasma density and temperature increase as the beam particles and energy are absorbed by the target plasma. At the initial target-plasma conditions a large fraction of the iron (or Ti, Ni, etc.) atoms near the plasma center are expected to be in the heliumlike state. Thus, the observed beam-induced increase of the lithiumlike state concentration is ascribed⁴ largely to recombination through charge exchange, e.g.,



or



etc., which must be sufficiently fast to overbalance the increasing ionization rates of Fe XXIV, Fe XXV, etc., due to the increased electron density and temperature. It is important to note that the increased radiation is ascribed to the lowering of the ionization balance, not to the recombination process *per se*.

The appropriate cross sections or rate coefficients for reactions (1a) and (1b) are not adequately known for the experimental beam velocities ($2 \times 10^8 \text{ cm/s}$ for D^0 injection), but the calculations of Olson and Salop,^{5,6} Grozdanov and Janev,⁷ and Duman and Smirnov⁸ indicate cross sections of 10^{-14} cm^2 or higher, which imply rate coefficients $(2-3) \times 10^{-6} \text{ cm}^3/\text{s}$. The ionization rate coefficients for Fe XXII–XXIV at $T_e \sim 2 \text{ keV}$ are of the order of $10^{-11} \text{ cm}^3/\text{s}$. Thus a neutral hydrogen to electron density ratio of $\sim 10^{-5}$ is indeed sufficient to significantly alter the ionization balance under the above mentioned experimental conditions.

The general effect on the radiation efficiency of iron atoms resulting from modification of coronal equilibrium charge-state distribution by additional recombination through charge exchange with atomic deuterium is shown in Fig. 2. These calculations⁹ assumed the charge-exchange cross sections of Olson and Salop⁶ for relative velocities appropriate to PLT neutral beam injections. Similar calculations have been performed¹⁰ for other elements and experimental conditions of interest. Clearly, the charge-exchange recombination under realistic neutral beam heating conditions has a significant effect on the tolerance limits of medium- Z elements in reactor-regime plasmas, with a temperature of about 10 keV.

Charge exchange with hydrogen atoms in tokamaks has been observed before in the recombination of fully stripped oxygen¹¹ during neutral beam

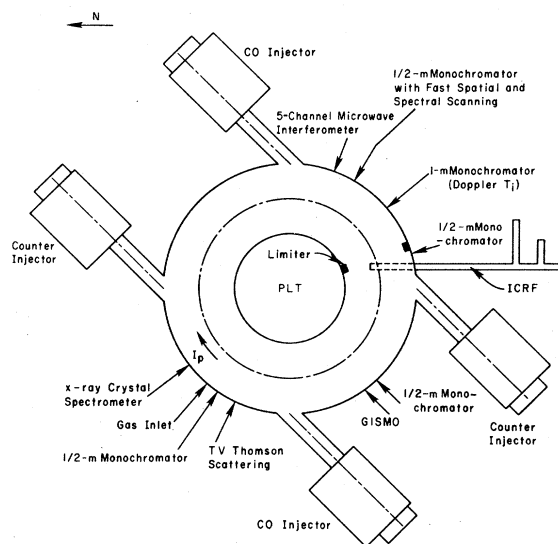


FIG. 1. Schematic view of the PLT tokamak showing location of the neutral beam and ion cyclotron resonance-frequency equipment and some of the diagnostic apparatus.

heating. The effect has also been employed to determine the concentration and time behavior of fully stripped carbon near the center of the discharge,¹² using an active diagnostic beam of hydrogen, rather than a high-power heating beam. In a similar fashion it will undoubtedly be possible to use the recombination for iron or titanium when the mechanism becomes more quantitatively

understood, both to study the space and time behavior of these ions, and also the energy and momentum deposition profiles of the heating beams.

In this paper we present experimental evidence for the charge-exchange recombination, comparing the space and time behavior of the lithiumlike iron and titanium ions with boronlike Fe XXII ion during neutral beam heating and ion cyclotron resonance-frequency (ICRF) heating, which has a similar effect on the plasma conditions but without introducing substantial quantities of additional neutral hydrogen into the discharge.

II. EXPERIMENTAL ARRANGEMENT

Figure 1 shows a plan view of the PLT tokamak with the associated neutral beam and ICRF heating and some of the relevant diagnostic equipment. The target plasma is generated by the toroidal current I_p , and lasts about 0.8 s in a quasisteady state. A carbon limiter at radius $a = 40$ cm and an iron limiter at radius 45 cm are used. The vacuum chamber wall (radius 50 cm) is covered with titanium by gettering. The four-beam lines then inject nominally 40-keV beams of H^0 or D^0 atoms, at about 500 kW each, for about 100 ms. The mean-free path of such atoms is about 60 cm, or slightly larger than the minor (limiter) radius of the plasma upon which they become ionized, mostly by charge exchange with plasma protons or collisions with electrons or protons, thereby raising the plasma temperature and density.^{1,2}

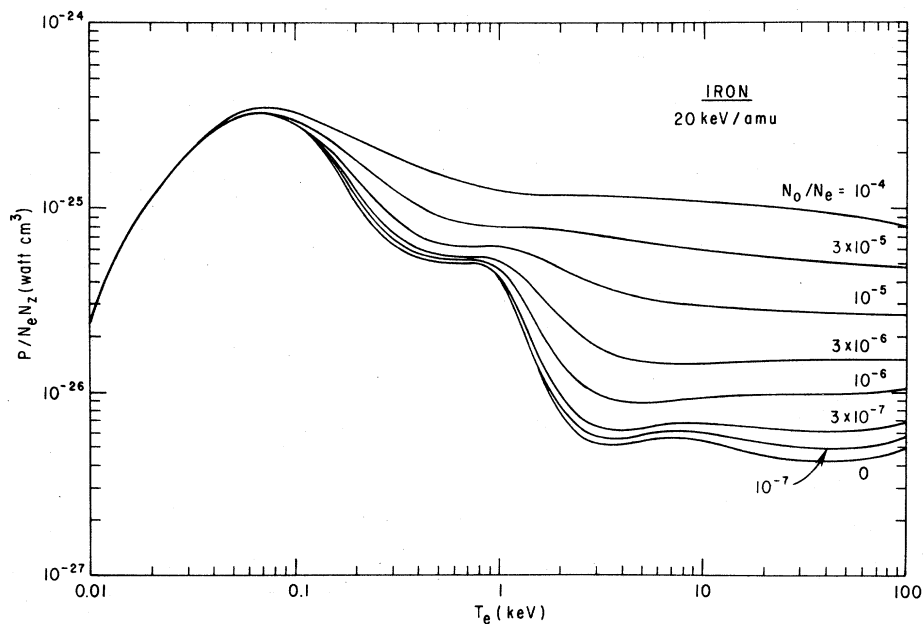


FIG. 2. Emissive power per iron atom in a plasma at electron temperature T_e , with coronal equilibrium ionization balance modified by charge-exchange recombination due to different neutral hydrogen to electron density ratio N_0/N_e .

Thus, the beam-atom density is high only between the injector pairs, or about over $\frac{1}{4}$ of the torus. However, the toroidal mobility of the ions is sufficiently large to permit consideration of toroidal averages only.

The line intensities in the range 40–1200 Å were measured with the grazing incidence spectrometer monochromator (GISMO), with radial (chord) distributions determined from shot-to-shot measurements. At longer wavelengths the intensities were measured with a 0.5-m Czerny-Turner monochromator equipped with a rotating mirror system to allow single-shot repeated spatial scans. The Fe XXV 1.85-Å line intensity was measured with a high-resolution crystal spectrometer¹³ in the equatorial plane only. The radial profiles of electron density and temperature were determined from a 5-channel 2-mm-microwave interferometer and the ruby laser Thomson scattering system.¹⁴ The former gives a continuous chord measurement of the density, and the latter an instantaneous radial profile of $T_e(r)$ and $N_e(r)$, with time evolution constructed from shot-to-shot measurements.

Before discussing the results, we note that (a) the hydrogen target plasma generally contains about 0.1% of Fe and somewhat lesser quantities of Ti, Cr, and Ni (as well as ~1% oxygen and carbon, which may be ignored for the present purposes) (b) the amounts of metal impurities depend on the plasma conditions but do not vary appreciably during an ohmic heating discharge (c) it is not *a priori* known whether the effect of the neutral beam (or ICRF) is to change the amount of metallic impurities in either direction (d) the radial transit time for the ions from the periphery to the center or back is typically 20–40 ms, and (e) a coronal equilibrium charge-state distribution [corresponding to observed $T_e(r)$] cannot be assumed with or without the neutral beam injection.

III. RESULTS AND INTERPRETATIONS

Figure 3 shows a representative sample of the observed ion-line intensities during a four-beam 2.1-MW D^0 injection into a hydrogen target plasma, with the changes of the central electron density and temperature indicated at the lower graph. The emissivity of the 1.85-Å line of Fe XXV (with excitation energy 6.6 keV) is a strongly increasing function of the electron temperature, whereas the other line emissivities are practically independent of temperature. The emissivities increase linearly with electron density, except for the (forbidden) 846-Å line of Fe XXII, which increases somewhat less than linearly in the density

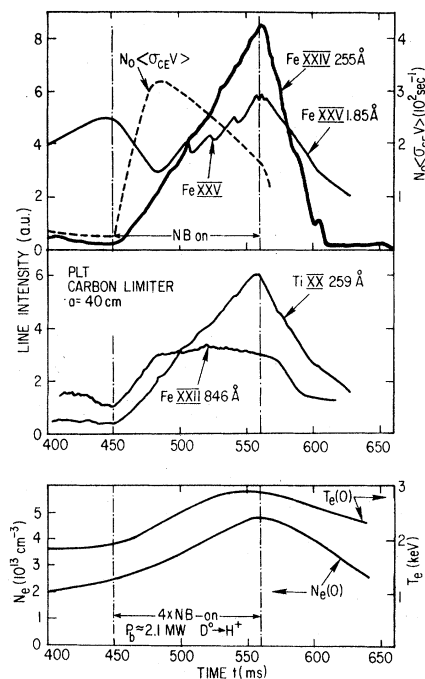


FIG. 3. Time evolution of Fe XXIV, Fe XXV, Fe XXII, and Ti XX line intensities during neutral beam (NB) injection. Dashed curve represents rate of charge exchange of Fe XXV and D^0 . Central electron temperature $T_e(0)$ and density $N_e(0)$ are shown in lower part of the figure.

range under consideration. The quantity $N_0 \langle \sigma_{ce} v \rangle$ in the upper graph is the estimated rate of charge exchange of Fe XXV [Eq. (1a)]. The neutral deuterium density N_0 is calculated from the measured neutral beam intensity, and includes slow-down and thermal atoms (i.e., recycled atoms heated by further charge exchange near the plasma periphery), all averaged over the toroidal circumference.

As the estimated charge-exchange rate increases (450–490 ms), there is a substantial drop of the Fe XXV line emission in spite of the increasing temperature and density, indicating a large decrease of the heliumlike iron ion density. As the electron density increases, the charge-exchange rate drops because of reduced penetration of neutral atoms (especially the thermal component). The 1.85-Å emissivity then increases, apparently mostly because of the continued increase of $T_e(0)$ (i.e., the observed emission corresponds to a roughly constant Fe XXV density from 500–600 ms). The lithiumlike Fe XXIV 255-Å emissivity rises strongly throughout the injection period, much faster than the rise in electron density, indicating a considerable increase in the Fe XXIV–XXV collisional ionization rate,

which should decrease the Fe XXIV density. The lithiumlike Ti XX shows qualitatively similar behavior to Fe XXIV although its ionization potential is significantly smaller and the relevant ionization rates larger, which probably accounts for the more gradual relative changes of intensity. However, the behavior of the Fe XXII ion, with ionization potential between Fe XXIV and Ti XX, is quite different; the relative rise is much less, and the intensity remains nearly constant after about 40 ms. The different behavior is not somehow connected with the 846-Å line (used here because of its convenient wavelength) due to a forbidden transition; the resonance lines of Fe XXII behave quite similarly. Furthermore, all observed ion lines below the boronlike state, both Fe and Ti, resemble the Fe XXII, whereas the berylliumlike Fe XXIII and Ti XIX are similar to the lithiumlike ions, except for quantitative details. Thus there is a clear indication of a general lowering of the dominant ionization stage from heliumlike to lithium or berylliumlike states during the beam injection, although the process is complicated by concomitant changes in the plasma conditions. After the beam pulse, there appears to be a restoration of the initial conditions on a time scale commensurate with the relaxation of the electron density and temperature.

Figure 4 shows an approximate computer calculation of the iron ion densities, using experimental electron densities and temperatures, and the charge-exchange rate $N_0 \langle \sigma_{ce} v \rangle$ shown in Fig. 3. In order to reproduce the observed time evolution of the Fe XXII ion, the total iron concentration was augmented by additional influx of iron, as shown. The resulting time behavior of Fe XXIV and XXV, mostly caused by the charge-exchange recombination (but also significantly affected by the influx term), is qualitatively similar to the

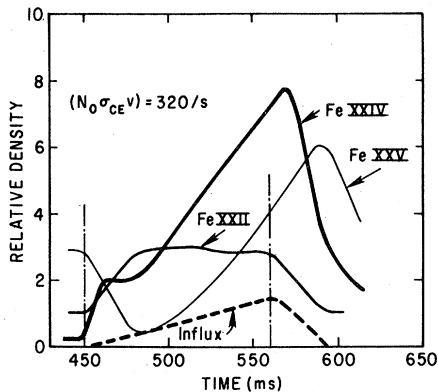


FIG. 4. Calculated time evolution of Fe XXIV and Fe XXV densities. Iron influx rate (dashed curve) was chosen to satisfy observed change of Fe XXII line intensity.

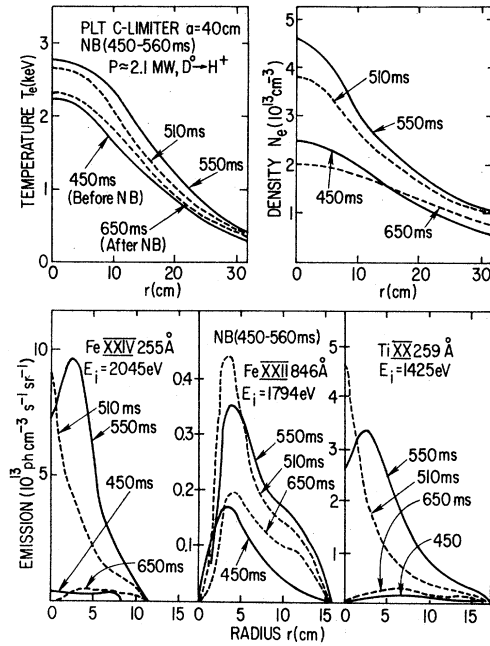


FIG. 5. Radial profiles of Fe XXIV, Fe XXII, and Ti XX line intensities and the electron temperature and density before (450 ms), during (510 and 550 ms), and after (650 ms) neutral beam injection.

observed changes in Fig. 3. However, because of the gross oversimplifications in the (zero-dimensional) computer code, and the many uncertainties in the experimental conditions, particularly regarding radial transport rates, more detailed correlations are not warranted at present.

Figure 5 shows the measured radial profiles of the emissivities of the Fe XXIV, XXII, and

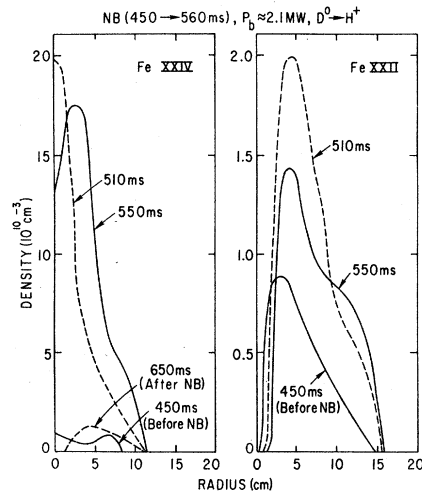


FIG. 6. Radial profiles of Fe XXIV and Fe XXII ion densities, corresponding intensity profiles from Fig. 5.

TiXX lines, and the electron density and temperature before (450 ms), during (510 and 550 ms), and after (650 ms) the neutral beam injection. Before the injection the intensities were of comparable magnitude (note differences in scales) with the peak emissivities of the lower ionization potential FeXXII and TiXX ions successively further outward. However, at 510 ms (60 ms after start of injection) the emissivities of the lithium-like FeXXIV and TiXX lines are strongly peaked in the center, with intensities over 20 times pre-injection values, whereas the FeXXII emissivity changes much less dramatically both in shape and magnitude. By 550 ms the emissivity of the lithi-

unlike ions has continued to grow at larger radii, but there is a significant relative decrease in the center. In explaining such changes, possible depletion of the heliumlike states as well as the decrease of the neutral hydrogen density and the increase of ionization rates due to changes in electron temperature and density may be important. At 650 ms the radial profiles of all three lines have reverted to more or less the pre-injection state.

The absolute ion densities deduced from the measured emissivities of Fig. 5 are shown in Fig. 6. The large magnitude of the change in the lithium-like ion density (with similar values for the

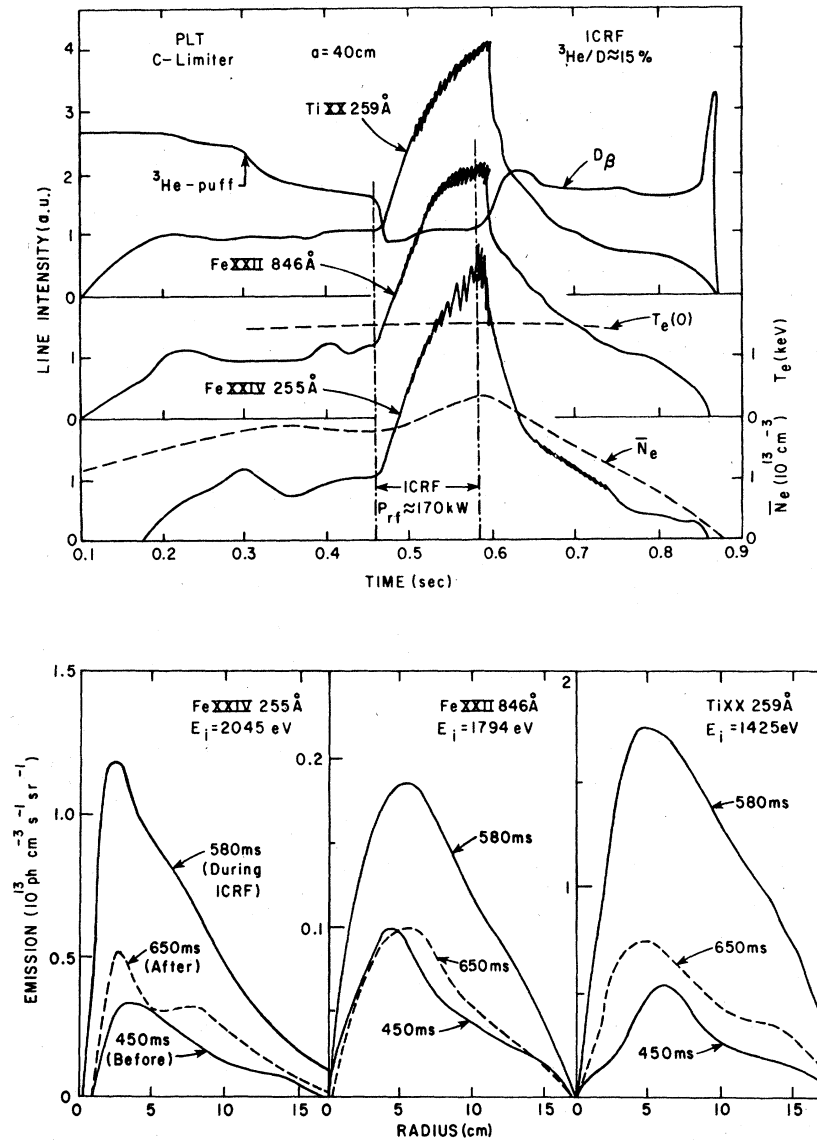


FIG. 7. Time evolution and radial distribution of FeXXIV, FeXXII, and TiXX line intensities during an ICRF heating experiment.

titanium ion), and the fact that the change first appears near the center and spreads outward, together with the constraints imposed on the iron influx rate by the behavior of FeXXII and other lower ionization states, indicate that the charge-exchange recombination must be the principal, although not the sole cause of the rearrangement of the ionization balance and the consequent changes in the radiation pattern during neutral beam injection.

A quite different picture of the lithiumlike ion behavior appears during ICRF auxiliary heating,¹⁵ as shown in Fig. 7. In this experiment the wave energy was coupled preferentially to a 15% $^3\text{H}_e^{++}$ component admixed to the plasma and the heating proceeds by collisional coupling of these superthermal helium ions with the bulk of the plasma. Thus, superthermal D^0 atoms were not present in appreciable quantities, and changes in the thermal component due to increased ion temperature have only a minor effect in increasing the neutral hydrogen density near the center of the discharge. There were only small changes in electron densities and temperatures. The intensities of the three ions increased by a similar amount, roughly comparable to the Fe XXII change in the neutral beam experiment. The 1.85-Å line of Fe XXV (not shown) also increased in a rather similar fashion. The radial emissivity profiles remained fairly constant in shape, with peak emissivities ordered according to ionization potential. All these changes can be attributed to an increased iron influx during the auxiliary heating, roughly comparable to that occurring during the neutral beam heating, but with no significant change in the recombination (or ionization) rates.

IV. DISCUSSION AND CONCLUSIONS

The experimental evidence for the importance of the charge-exchange recombination is essentially twofold: (1) The simultaneous decrease of Fe XXV light and increase of the Fe XXIV light (Fig. 3) at a time where the increased ionization rate (increased T_e and N_e) should lead to the opposite behavior, and (2) the essentially different space behavior of TiXX and Fe XXII, with comparable ionization rates, during the neutral beam injection. Either of these effects appear to be impossible to explain on the basis of plasma dynamics, e.g., changes of radial particle transport rates resulting from possible changes of the current density distribution and of magnetic field topology. The evidence is further reinforced by the fact that realistic estimates of the charge-exchange cross sections and the neutral hydrogen density near the center of the discharge are suf-

ficient to account for the observed effects.

However, there is no lack of difficulties with simple explanations. The production of the lithiumlike ions through charge exchange should have a radial distribution that is the convolution of the heliumlike ion and the neutral hydrogen density. The narrowness (and height) of the observed lithiumlike ion profiles, especially during the early part of the beam injection, is therefore rather startling. Although there are no direct measurements of the heliumlike ion profiles, there is no reason to expect that these in particular should be strongly concentrated near the center. Quite to the contrary, because of their relatively long recombination times (i.e., radiative and dielectronic recombination in the ohmically heated target plasma) and very long ionization times, their radial profiles should be fairly wide, probably considerably wider than those of the (directly observable) lithiumlike ions. Nor can the neutral hydrogen density be narrowly concentrated in the center—in comparison with the observed profiles it should be practically uniform in radius. [There are still other mysterious effects, not discussed in the present paper. Thus, in unbalanced beam injection, e.g., 3 beams or 2 beams in the same direction, often large amplitude (>50%) fairly regular ("sawtooth") oscillations occur in some of the ion densities, especially near the center of the discharge, indicating rapid periodic changes in plasma conditions. A mild form of such oscillations is shown in Fig. 7 during the ICRF heating and also in the Fe XXV line in Fig. 3. This phenomenon will be discussed in future reports when more systematic measurements become available.]

We therefore conclude that, while charge-exchange recombination is a principal cause of the observed ion-density behavior during the beam injection, there are other presumably plasma-dynamic effects of comparable importance involved. Because of the obvious implications of these processes for beam-driven reactor-type plasma devices, as well as their intrinsic interest both in plasma physics and atomic physics, this phenomenon deserves thorough experimental study, including built-in redundancies by the use of different ions (e.g., Cr, Ni, and Kr in addition to Ti and Fe), complemented by modeling calculations that include radial profiles and particle transport rates.

ACKNOWLEDGMENTS

The authors are very grateful to Dr. K. Bol, Dr. N. Bretz, Dr. D. Dimock, Dr. H. Eubank,

Dr. R. Fonck, Dr. R. Goldston, Dr. R. Hawryluk,
Dr. J. Hosea, Dr. F. Jobes, Dr. D. Johnson, Dr.
E. Meservey, Dr. J. Strachan and Dr. W. Stodiek

for support and help in experiments. This work
was supported by the U. S. Department of Energy
Contract No. De-AC02-76-CHO-3073.

¹H. Eubank *et al.*, in *Proceedings of the 7th International Conference on Plasma Physics and Controlled Nuclear Fusion Research*, Innsbruck, Austria, 1978 (IAEA, Vienna, Austria, 1979).

²H. Eubank *et al.*, *Phys. Rev. Lett.* **43**, 270 (1979).

³E. Hinnov and S. Suckewer, *Bull. Am. Phys. Soc.* **24**, 767 (1979); E. Hinnov, *Astrop. J.* **230**, L197 (1979).

⁴E. Hinnov, *Proceedings of the U.S.-Japan Joint Seminar on Plasma Spectroscopy* (Kyoto University, Kyoto, Japan, 1979).

⁵R. E. Olson and A. Salop, *Phys. Rev. A* **14**, 579 (1976).

⁶R. E. Olson and A. Salop, *Phys. Rev. A* **16**, 531 (1977).

⁷T. P. Grozdanov and R. K. Janev, *Phys. Rev. A* **17**, 880 (1978).

⁸E. L. Duman and B. M. Smirnov, *Fiz. Plazmy* **4**, 1161 (1978) [*Sov. J. Plasma Phys.* **4**, 650 (1978)].

⁹D. E. Post, R. A. Hulse, E. Hinnov, and S. Suckewer, in *Proceedings of the Eleventh International Conference on the Physics of Electron and Atomic Collisions* (Ky-

oto, Japan, 1979).

¹⁰R. A. Hulse, D. E. Post, and C. B. Tarter, *Bull. Am. Phys. Soc.* **24**, 767 (1979); R. A. Hulse, D. E. Post, and D. R. Mikkelsen, Princeton University, Plasma Physics Laboratory Report No. PPPL-1633 (unpublished).

¹¹R. C. Isler, *Phys. Rev. Lett.* **38**, 1359 (1977); R. C. Isler and E. C. Crume, *ibid.* **41**, 1296 (1978).

¹²V. V. Afrosimov, Y. S. Gordeev, A. N. Zinoviev, and A. A. Korotkov, *Zh. Eksp. Teor. Fiz. Pis'ma Red.* **28**, 505 (1978) [*JETP Lett.* **28**, 500 (1978)].

¹³M. Bitter *et al.*, *Phys. Rev. Lett.* **42**, 304 (1979).

¹⁴N. Bretz, D. Dimock, V. Foote, D. Johnson, D. Long, and E. Tolnas, *Appl. Opt.* **17**, 198 (1978).

¹⁵J. Hosea *et al.*, *Course and Workshop on Physics of Plasmas Close to Thermonuclear Condition*, Varenna, Italy, 1979 (Editrice Compositori, Bologna, Italy, 1980).